Optimization of Penalized Block-iterative Algorithms for Ga-67 Tumor Detection

H.C. Gifford[1], C.L. Byrne[2], M.V. Narayanan[1], and M.A. King[1]
[1]Department of Radiology, University of Massachusetts Medical School, Worcester, MA, 01655, USA
[2]Department of Mathematics, University of Massachusetts-Lowell, Lowell, MA, 01854, USA

Abstract— **Our purpose is to optimize penalized block-iterative algorithms for detection of Ga-67 tumors in the thorax. We illustrate some of our methods involving psychophysical studies with results from a preliminary channelized Hotelling observer (CHO) optimization for a one-step-late (OSL) version of the penalized RBI-EM algorithm that features a 3D uniform quadratic penalty function. The algorithm parameters to be optimized are iteration number and a penalty weighting parameter β. Use of the CHO is an efficient means of bounding regions of parameter space that contain the optimal parameters, although the final determination of the optimal parameters will be left to human psychophysical studies. From the CHO optimization, we found that one iteration of the penalized RBI-EM algorithm could outperform a previously optimized reconstruction strategy with RBI-EM and post-filtering that required three iterations.**

I. INTRODUCTION

By most definitions of image quality, unregularized reconstructions of SPECT data are substandard. Procedures for improving the quality of iterative reconstructions usually involve penalty functions, stopping rules, and post-reconstruction filters. Whether a particular regularization scheme actually improves an image will depend on one's image quality measure. In a series of earlier papers [1-3], we documented optimizations of the ordered-sets expectation-maximization (OSEM) [4] and rescaled block-iterative EM (RBI-EM) [5] algorithms that were aimed at determining if detection of Ga-67 tumors in the thorax could be improved by modeling the physics of the data acquisition in the inverse problem. These algorithms used a post-reconstruction Gaussian filter as a regularizer. This current abstract describes the early stages of similar optimizations of algorithms derived by incorporating 3D penalty-function regularizers into the RBI-EM algorithm and the block-iterative interior point algorithm (IPA) [6]. Such penalized-likelihood methods are often viewed in the context of maximum a posteriori (MAP) reconstruction [7].

One motivation for investigating these penalized algorithms comes from the results of our work with the OSEM and RBI-EM algorithms. Based on detection-performance metrics drawn from localization ROC (LROC) [8] studies with human observers, it was determined [2] that the OSEM algorithm with nonuniform attenuation correction (AC) and three-dimensional (3D) detector-response correction (DRC) did improve detection in comparison to the OSEM algorithm with only AC or with neither correction. Even so, it was also seen that a significant difference in performance existed between our DRC reconstructions and "ideal" reconstructions that represented an upper bound on DRC. The Gaussian post-filter may have contributed to this difference by partially negating the effect of the DRC in our reconstructions. If this were true, we might expect to find that regularization with edge-preserving penalty functions [7, 9] boosts observer performance over that obtained with the post-filter regularization.

To show that one algorithm offers improvement over another in a fair comparison first requires optimization of each algorithm with respect to its adjustable parameters. We perform these preliminary optimizations using a combination of channelized Hotelling observer (CHO) [10] ROC and human-observer LROC studies. Use of the CHO offers an efficient means of coarsely bounding regions of parameter space that contain the optimal parameters. The actual determination of those optimal parameters is then left to the LROC studies, but the workload for the human observers is reduced by having applied the CHO. In this abstract, we illustrate this approach with results from a preliminary CHO optimization for a one-step-late (OSL) version of the penalized RBI-EM algorithm that features a 3D uniform quadratic penalty function. The adjustable parameters to be optimized in this case are iteration number and a penalty weighting parameter β. This penalty function does not have edge-preserving characteristics, but allows comparison to our past studies with the Gaussian post-filter. Edge-preserving penalty functions are also to be investigated for use with the penalized RBI-EM and IPA algorithms. The inclusion of the penalized IPA algorithm in this research provides a reconstruction method that is not based on the OSL approximation.

II. METHODS

A. The Phantom

A distribution of Ga-67 citrate in the chest was simulated with one geometry of the 3D mathematical cardiac-torso (MCAT) phantom [11]. Background activity levels in the phantom were set by reference to clinical values. Tumors were modeled as 1-cm diameter spheres with a tumor-to-soft-tissue activity ratio of 20:1. Each "abnormal" case contained one tumor, randomly placed within a 3D map of likely tumor areas.

B. The Projection Data

Separate analytic projections of the phantom and tumors were created and then combined into a noise-free tumor-present projection sets. The projector modeled nonuniform attenuation in the phantom and the response for a medium-energy parallel-hole collimator. For the results presented herein, perfect scatter rejection was assumed so that comparisons with our previous optimizations of OSEM and RBI-EM could be made, but simulations that include scatter are also being done. Separate projections for 93- and 185-keV photons were obtained using energy-specific atten-

uation maps, and then added as a weighted sum based on the relative abundances and camera efficiencies for these energies. Projection sets consisted of 128 256×256 projections (pixel width of 0.1585 cm), rebinned to 128×128 pixels (pixel width of 0.317 cm). Poisson noise was added to form data sets of 8 million counts.

C. The Reconstruction Algorithm

For this abstract, we consider a OSL penalized version of the RBI-EM algorithm [5]. Like the OSEM algorithm, the RBI-EM algorithm is a block-iterative version of the maximum-likelihood expectation maximization (MLEM) algorithm, but unlike the OSEM algorithm, it converges in the case of consistent data for any choice of subsets. Our human-observer LROC studies have also shown that the RBI-EM algorithm is more robust than the OSEM algorithm as the number of projection data subsets is increased in order to accelerate the reconstruction [3]. To define the penalized RBI-EM algorithm, we let $\hat{\mathbf{f}}^{(j)}$ be the j^{th} iteration ($j = 0, ..., \infty$) of $\mathbf{f}$, with individual elements $\hat{f}_n^{(j)}$, and consider the detector pixels divided into R disjoint subsets $S_1, \ldots, S_R$. The convention followed here is that every cycle through the R subsets represents an iteration. An RBI-EM algorithm regularized with penalty function $U(\hat{\mathbf{f}}^{(j)})$ requires solving the equation

$$\hat{f}_n^{(j+1)} = \frac{\hat{f}_n^{(j)}}{\sum_m H_{mn} + \beta \frac{\partial U(\hat{\mathbf{f}}^{(j+1)})}{\partial \hat{f}_n^{(j+1)}}} \times \left[\sum_m H_{mn} + a_r{}^{-1} \left(\sum_{m \in S_r} H_{mn} \left(\frac{g_m}{[\mathbf{H}\hat{\mathbf{f}}^{(j)}]_m} - 1\right)\right)\right], \tag{1}$$

for $\hat{f}_n^{(j+1)}$, where $r = (j \bmod R) + 1$, β is the nonnegative penalty weight, and

$$a_r \equiv \max_n \left(\sum_{m \in S_r} H_{mn} / \sum_m H_{mn} \right). \tag{2}$$

For arbitrary U, a closed-form expression for $\hat{f}_n^{(j+1)}$ is unobtainable from Eq. (1). One way around this difficulty is to replace $U(\hat{\mathbf{f}}^{(j+1)})$ with $U(\hat{\mathbf{f}}^{(j)})$, which is referred to as the OSL approach [7].

Our uniform quadratic penalty function has the form

$$U(\hat{\mathbf{f}}^{(j)}) = \frac{1}{2} \sum_{k \in V} \sum_{i \in N_k} w_{ik} (\hat{f}_k^{(j)} - \hat{f}_i^{(j)})^2, \tag{3}$$

where V is the full set of voxels in the 3D reconstruction, N_k represents the $3 \times 3 \times 3$ cube of voxels centered about the k^{th} voxel, and w_{ik} is the distance between the centers of the k^{th} and i^{th} voxels in N_k, normalized by the voxel width. The optimization parameters for this choice of U are the number of iterations and the magnitude of β. Each combination of iteration number and β shall be referred to as a reconstruction strategy. For a point of comparison, our past studies [3] found optimal observer detection performance with 3 iterations (32 subsets of 4 projection angles each) of the RBI-EM algorithm combined with a 3D Gaussian post-filter with a FWHM of 0.95 cm.

Reconstructions with matrix dimensions of $128 \times 128 \times 128$ were obtained with strategies using one iteration of Eq. (1) and four projection angles per subset for values of β between 0.0 and 1.5. Both the AC and the DRC procedures that had been used in [2] were included in the iteration. The attenuation map used for the AC was the same one used in the creation of the projection sets, and in that sense was an optimal attenuation correction [12]. No post-reconstruction filter was applied. For LROC studies, 2D images through the center of the tumor are extracted from the 3D reconstructions. These are then adaptively thresholded, interpolated to 256×256 pixels, and then converted from floating-point to byte images for display to the human observers. For the CHO, the same 2D slices were extracted, but the thresholding, interpolation, and conversion to greyscales were not applied. Excluding these steps reduced the computing time and also allowed use of a low-noise approximation for constructing the CHO that is described in Section II-D. For OSEM-reconstructed images, we have found [13] that omitting these processes has little impact on the correlation between the CHO and average human observer.

D. Observer Studies

Our evaluation of reconstruction algorithms uses LROC methodology to measure human-observer performance of the Ga-67 tumor detection task. In a standard ROC study, an observer's response for an image is a confidence rating that a tumor is either present or absent. For an LROC study, the observer is asked to give this confidence rating and the coordinates of the maximally suspicious tumor location. By implementing this detection and localization task, LROC offers both a better approximation of clinical detection tasks and increased statistical accuracy over ROC for measuring detection performance [8]. With this improvement in accuracy comes increased statistical power for discriminating between reconstruction strategies.

The CHO is a linear discriminant function that has been shown [14-18] to correlate with humans for many "signal-known-exactly" (SKE) detection tasks, in which the observer knows the tumor location from the outset. We do not yet have a modified version of the CHO that can perform the search and detection task associated with these LROC studies and still correlate with humans, but we have found that the average CHO performance in series of SKE-ROC studies with multiple tumor location agrees with average human performance in the sense that both indicate similar significant differences between reconstruction strategies [3, 13, 19].

For a given tumor location, the response of the CHO to an image is a scalar λ that is a weighted sum of the image voxels. This sum can be viewed as the inner product between the image and a template image $\mathbf{w}_{\text{cho}}$. Let $\hat{\mathbf{f}}$ be a 3D reconstruction from noisy data that, with equal likelihood, comes from an ensemble $\mathcal{H}_0$ of tumor-absent reconstructions or an ensemble $\mathcal{H}_1$ of tumor-present reconstructions. Post-reconstruction processing such as extraction of the transaxial slice of interest is performed by opera-

tor $\mathcal{S}$, so that $\mathcal{S}\hat{\mathbf{f}}$ is a 2D image intended for the observer. Then $\lambda = \mathbf{w}_{\text{cho}}^{\dagger}\mathcal{S}\hat{\mathbf{f}}$, where the † indicates a vector transpose. Comparison of λ to a threshold value determines whether the CHO decides the image contains a tumor. The CHO's overall performance can be quantified by a signal-to-noise ratio for λ [20],

$$\text{SNR}^2 = \frac{\left[\langle\lambda|\mathcal{H}_1\rangle - \langle\lambda|\mathcal{H}_0\rangle\right]^2}{\frac{1}{2}\text{var}(\lambda|\mathcal{H}_1) + \frac{1}{2}\text{var}(\lambda|\mathcal{H}_0)}, \tag{4}$$

where $\langle\lambda|\mathcal{H}_i\rangle$ and $\text{var}(\lambda|\mathcal{H}_i)$ $(i = 0, 1)$ are the mean and the variance of the distribution of λ for the i^{th} ensemble.

The CHO template is composed of a matrix $\mathbf{U}$ of impulse responses for a set of C 2D prefilters (the "channels") centered on the tumor location, a channel covariance matrix $\mathbf{K}_{\text{chan}}$, and a matched filter. For ensemble $\mathcal{H}_i$, let $\bar{\hat{\mathbf{f}}}_i$ be the mean 3D reconstruction and let $\mathbf{K}_i$ be the voxel covariance matrix. Assuming $\mathcal{S}$ applies only linear post-processing, we make the definition

$$\mathbf{K}_{\text{chan}} = \frac{1}{2}\mathbf{U}\mathcal{S}[\mathbf{K}_0 + \mathbf{K}_1]\mathcal{S}^{\dagger}\mathbf{U}^{\dagger}, \tag{5}$$

and express the CHO template as [10]

$$\mathbf{w}_{\text{cho}} = \mathbf{U}^{\dagger}\mathbf{K}_{\text{chan}}^{-1}\mathbf{U}\mathcal{S}(\bar{\hat{\mathbf{f}}}_1 - \bar{\hat{\mathbf{f}}}_0). \tag{6}$$

Substituting Eq. (6) into Eq. (4) leads to the formula

$$\text{SNR}_{\text{cho}} = \left[(\bar{\hat{\mathbf{f}}}_1 - \bar{\hat{\mathbf{f}}}_0)^{\dagger}\mathcal{S}^{\dagger}\mathbf{U}^{\dagger}\mathbf{K}_{\text{chan}}^{-1}\mathbf{U}\mathcal{S}(\bar{\hat{\mathbf{f}}}_1 - \bar{\hat{\mathbf{f}}}_0)\right]^{\frac{1}{2}} \tag{7}$$

for evaluating the CHO's performance.

The channel covariance and matched-filter portions of the CHO require knowledge of the ensemble statistics of $\mathcal{H}_0$ and $\mathcal{H}_1$, and determining these statistics accounts for the computational expense of using the CHO. Oftentimes, sets of noisy reconstructions are generated to produce sample statistics. In doing so, one makes use of the fact that the number of channels C (C=3 in our CHO model) is much smaller than the number of image voxels by computing $\mathbf{K}_{\text{chan}}$ directly from the $C \times C$ "channelized" images $\mathbf{U}\mathcal{S}\hat{\mathbf{f}}$ instead of estimating $\mathbf{K}_i$ in full. For complex iterative reconstruction algorithms, this approach is very computationally intensive [21]. An alternative is to make a low-noise assumption about the images [22-24] and thus approximate the ensemble statistics by a recursive procedure using noise-free data. Let $\hat{\mathbf{f}}^{(k)} \in \mathcal{H}_i$ be the k^{th} iteration with $\mathbf{g}$, and let $\mathbf{a}^{(k)}$ be the k^{th} iteration with the noise-free data $\overline{\mathbf{g}}$. Also, define $\mathbf{D}^{(k)}$ as the diagonal matrix with element $D_{jj}^{(k)} = a_j^{(k)}$, the j^{th} element of $\mathbf{a}^{(k)}$. When $\hat{\mathbf{f}}^{(k)} \approx \mathbf{a}^{(k)} + \boldsymbol{\epsilon}^{(k)}$ for small perturbations $\boldsymbol{\epsilon}^{(k)}$, then $\bar{\hat{\mathbf{f}}}_i \approx \mathbf{a}^{(k)}$ [22], and

$$\mathbf{K}_i \approx \mathbf{D}^{(k)}\ \mathbf{O}^{(k)}\ \mathbf{K}_g\ [\mathbf{O}^{(k)}]^{\dagger}\ \mathbf{D}^{(k)}. \tag{8}$$

The matrix $\mathbf{O}^{(k)}$ describes how noise in the data is transferred into the reconstruction through k iterations. We determined the specific form of $\mathbf{O}^{(k)}$ for the penalized RBI-EM algorithm by merging the results in [24] for MAP-type reconstuction algorithms with [22], which treats block-iterative methods such as the RBI-EM algorithm. As with the sample statistics approach described above, the channel covariance should be calculated directly by computing the product $\mathbf{A}^{\dagger}\mathbf{A}$, where

$$\mathbf{A} = \mathbf{K}_g^{\frac{1}{2}}[\mathbf{O}^{(k)}]^{\dagger}\mathbf{D}^{(k)}\mathcal{S}^{\dagger}\mathbf{U}^{\dagger}. \tag{9}$$

The SKE-ROC studies were conducted for 5 tumor locations. The overall CHO performance for a strategy was figured by converting SNR_{cho} for each location into an area under the ROC curve A_Z as described in [19] and then computing the average area $\langle\text{A}_\text{Z}\rangle$ over location. The computation time required to evaluate SNR_{cho} for a given strategy at a single location is on the order of the time required to perform $2(C + 1)$ reconstructions with that strategy.

III. RESULTS AND CONCLUSIONS

The results of the ROC studies are presented in Figure 1, in which $\langle\text{A}_\text{Z}\rangle$ is plotted against β for the penalized RBI-EM strategies that used a subset size of four angles per subset. The high values of $\langle\text{A}_\text{Z}\rangle$ seen for these ROC studies are partly due to the fact that the tumor contrast and the number of counts in the data sets were originally set for use in the LROC studies.

The solid horizontal line at $\langle\text{A}_\text{Z}\rangle \approx 0.98$ denotes the CHO performance using three iterations of the RBI-EM algorithm and a 3D Gaussian post-filter of FWHM = 0.95 cm. The best-performing ($\langle\text{A}_\text{Z}\rangle \approx 0.99$) of the strategies we tested used β=1.25, but several other strategies also outperformed the RBI-EM strategy. The effect on CHO performance of using more iterations and different numbers of subsets is currently being investigated. Also, whether the precipitous fall-off in performance above β=1.25 will find a correlation in human LROC studies remains to be seen.

IV. ACKNOWLEDGEMENTS

This work was supported in part by the National Cancer Institute (NCI) under grant number CA-42165.

References

[1] R G Wells, M A King, P Simkin, P Judy, A B Brill, H C Gifford, R Licho, P H Pretorius, P Schneider, and D W Seldin, "Comparing FBP and OSEM for small lesion detection and localization in Ga-67 SPECT," *J. Nucl. Med.*, vol. 41, pp. 1391–1399, 2000.

[2] H C Gifford, M A King, R G Wells, W G Hawkins, M V Narayanan, and P H Pretorius, "LROC analysis of detector-response compensation in SPECT imaging," *IEEE Trans. Med. Imaging*, vol. 19, pp. 463–473, 2000.

[3] H C Gifford, R G Wells, and M A King, "Effect of block-iterative acceleration on Ga-67 tumor detection in thoracic SPECT," *IEEE Trans. Nucl. Sci.*, (submitted).

[4] H M Hudson and R S Larkin, "Accelerated image reconstruction using ordered subsets of projection data," *IEEE Trans. Med. Imaging*, vol. 13, pp. 601–609, 1994.

[5] C L Byrne, "Block-iterative methods for image reconstruction from projections," *IEEE Trans. Imag. Proc.*, vol. 5, pp. 792–794, 1996.

[6] C L Byrne, "Block-iterative interior point optimization methods for image reconstruction from limited data," *Inverse Problems*, vol. 16, pp. 1405–1419, 2000.

[7] P J Green, "Bayesian reconstructions from emission tomography data using a modified EM algorithm," *IEEE Trans. Med. Imaging*, vol. 9, pp. 84–93, 1990.

[8] R G Swensson, "Unified measurement of observer performance in detecting and localizing target objects on images," *Med. Phys.*, vol. 23, pp. 1709–1725, 1996.

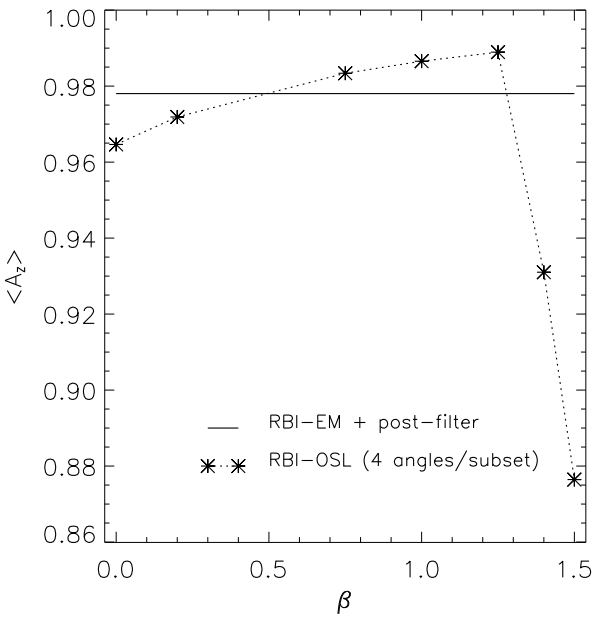

Fig. 1. A plot of$\langle A_Z \rangle$ versus β for the penalized RBI-EM strategies with one iteration and four angles per subset. The horizontal line denotes CHO performance using the RBI-EM algorithm and post-filtering.

[9] D S Lalush and B M W Tsui, "Simulation evaluation of Gibbs prior distributions for use in maximum a posteriori SPECT reconstructions," *IEEE Trans. Med. Imaging*, vol. 11, pp. 267–275, 1992.

[10] K J Myers and H H Barrett, "Addition of a channel mechanism to the ideal-observer model," *J. Opt. Soc. Am. A*, vol. 4, pp. 2447–2457, 1987.

[11] B M W Tsui, X D Zhao, G K Gregoriou, J Li, D L Lalush, and R L Eisner, "Quantitative cardiac SPECT reconstruction with reduced image degradation due to patient anatomy," *IEEE Trans. Nucl. Sci.*, vol. 41, pp. 2838–2848, 1994.

[12] R G Wells, H C Gifford, P H Pretorius, T Farncombe, and M A King, "The impact of noisy attenuation maps and patient motion on human-observer performance at Ga-67 lesion detection in SPECT," in *2000 IEEE NSS-MIC Conference Record*, to appear.

[13] H C Gifford, E J Soares, R G Wells, and M A King, "Evaluating attenuation correction in Ga-67 SPECT image reconstruction through numerical observer ROC and human observer LROC," in *Proceedings of the 22nd Annual International Conference of the IEEE Engineering in Medicine and Biology Society*, 2000.

[14] J P Rolland and H H Barrett, "Effect of random background inhomogeneity on observer detection performance," *J. Opt. Soc. Am.*, vol. 9, pp. 649–658, 1992.

[15] C K Abbey, H H Barrett, and D W Wilson, "Observer signal-to-noise ratio for the ML-EM algorithm," *Proc. SPIE*, vol. 2712, pp. 47–58, 1996.

[16] M P Eckstein, C K Abbey, and J S Whiting, "Human vs. model observers in anatomical backgrounds," *Proc. SPIE*, vol. 3340, pp. 16–26, 1998.

[17] S D Wollenweber, B M W Tsui, E C Frey, D S Lalush, and K J LaCroix, "Comparison of human and channelized Hotelling observers in myocardial defect detection in SPECT," *J. Nucl. Med.*, vol. 39, pp. 170P, 1998 (abstract).

[18] H C Gifford, M A King, D J de Vries, and E J Soares, "Channelized Hotelling and human observer correlation for lesion detection in hepatic SPECT imaging," *J. Nucl. Med.*, vol. 41, pp. 514–521, 2000.

[19] H C Gifford, R G Wells, and M A King, "A comparison of human observer LROC and numerical observer ROC for tumor detection in SPECT images," *IEEE Trans. Nucl. Sci.*, vol. 46, pp. 1032–1037, 1999.

[20] H H Barrett, "Objective assessment of image quality: effects of quantum noise and object variability," *J. Opt. Soc. Am. A*, vol. 7, pp. 1266–1278, 1990.

[21] E C Frey, K J LaCroix, and B M W Tsui, "Application of task-based measures of image quality to optimization and evaluation of three-dimensional reconstruction-based scatter compensation in SPECT," in *Proc. Fully 3D Image Reconstruction in Radiology and Nuclear Medicine*, Egmond aan Zee, The Netherlands, 1999, pp. 289–291.

[22] E J Soares, C L Byrne, and S J Glick, "Noise characterization of block-iterative reconstruction algorithms: I. Theory," *IEEE Trans. Med. Imaging*, pp. 261–270, 2000.

[23] H H Barrett, D W Wilson, and B M W Tsui, "Noise properties of the EM algorithm: I. Theory," *Phys. Med. Biol.*, vol. 39, pp. 833–846, 1994.

[24] W Wang and G Gindi, "Noise analysis of MAP-EM algorithms for emission tomography," *Phys. Med. Biol.*, vol. 42, pp. 2215–2232, 1997.